Exact calculations of the relaxation for a model of electron transfer with strong electronic coupling

Masako Takasu
Department of Physics, Kanazawa University, Kakuma, Kanazawa 920-11 Japan
(Received 18 November 1994)

We study the short-time relaxation of a model of electron transfer with strong electronic coupling using exact enumeration of path-integral representation of population function. For asymmetric two-state systems, we find boundaries between phases of coherent and incoherent relaxation. We contrast the relaxation of the normal and inverted regions. In the normal region, the relaxation obeys the power law. In the inverted region, the relaxation is exponential. The rate constant in the inverted region is calculated. The effect of a third state is also investigated.

PACS number(s): 05.30.−d, 64.60.Cn, 73.40.Gk, 75.10.Jm

I. INTRODUCTION

In traditional treatments [1,2], the dynamics of electron transfer [3] is viewed in terms of incoherent and uncorrelated transitions between charge localized states. For large enough interstate coupling, however, transitions can be correlated in time and may also exhibit coherence. In this paper, we consider examples of correlations and coherence for a simple but realistic class of models. Specifically, we examine asymmetric two- and three-state systems coupled to a bath with linear Ohmic response. This class of models is discussed in Sec. II. It represents a generalization of the often studied spin-boson system [4,5]. Simulation studies have demonstrated that this type of model can well approximate the behavior of more detailed molecular models [6–10]. For a variety of cases, we carry out dynamical calculations through exact integration and explicit enumeration of quantum paths. The computation time for this type of calculations grows exponentially with the number of physical time steps. As such, we are limited to the length of time which can be studied. With reasonable computational resources, it is possible to examine correlation functions and relaxation for times as long as one or two tunneling periods. This length is sufficient to determine the phase boundary between coherent and incoherent relaxation and the effects of asymmetry on this boundary. In the incoherent regime, we are also able to estimate the functional form of the relaxation. Details of our computational procedure are given in Sec. III and the Appendixes. Results are presented in Sec. IV, and the paper is concluded in Sec. V.

II. MODEL

We investigate the following three-level system coupled to a bosonic bath:

$$H = H_0 + H_B + H_{\rm int}, \tag{2.1}$$

where H_0 is the bare Hamiltonian

$$H_0 = \begin{pmatrix} E_1 & J_{12} & J_{13} \\ J_{12} & E_2 & J_{23} \\ J_{13} & J_{23} & E_3 \end{pmatrix} \tag{2.2}$$

and H_B is the bath

$$H_B = \sum_j \left(\frac{p_j^2}{2m_j} + \frac{m_j \omega_j^2 x_j^2}{2} \right), \tag{2.3}$$

where p_j is the conjugate momentum of the normal mode x_j with mass m_j. The three states refer to charge localized states. As such, the effects of the fluctuating fields of an environment can be reasonably described through diagonal system-bath coupling. We assume that the fields are coupled to the diagonal elements of the three-level system. The case of the off-diagonal coupling is also of interest, but in this paper we deal only with the diagonal coupling. We also assume that the system-bath coupling is linear. The validity of the linear approximation for electron transfer, which underlies Marcus theory, has been established computationally [7]. Hence,

$$H_{\rm int} = \mathcal{E}_{12}\sigma_{12} + \mathcal{E}_{23}\sigma_{23} + \mathcal{E}_{13}\sigma_{13}. \tag{2.4}$$

Here, the σ_{ij}'s are

$$\sigma_{12} = \begin{pmatrix} 1 & 0 & 0 \\ 0 & -1 & 0 \\ 0 & 0 & 0 \end{pmatrix},$$

$$\sigma_{23} = \begin{pmatrix} 0 & 0 & 0 \\ 0 & 1 & 0 \\ 0 & 0 & -1 \end{pmatrix},$$

$$\sigma_{13} = \begin{pmatrix} -1 & 0 & 0 \\ 0 & 0 & 0 \\ 0 & 0 & 1 \end{pmatrix},$$

and $\mathcal{E}_k = \sum_j c_{jk} x_j$, where k runs over $A = (12)$, $B = (23)$, and $C = (13)$. The variables $\mathcal{E}_k$ are like local electric fields which couple to a charge transfer dipole. The behavior of the relevant bath variables is described

1063-651X/95/52(1)/418(10)/$06.00

by the spectral density

$$J_{kl}(\omega) = \frac{\pi}{2} \sum_j \frac{c_{jk} c_{jl}}{m_j \omega_j} \delta(\omega - \omega_j). \tag{2.5}$$

For electron transfer in complex systems such as liquids or proteins, the appropriate spectral density is Ohmic [7,11]. We choose the following function for the spectral density:

$$J_{kl}(\omega) = \eta_{kl} \omega \exp(-\omega/\omega_{kl}^{(c)}). \tag{2.6}$$

The dynamics of transitions between the charge localized states is the dynamics of electron transfer. One measure of it is the population autocorrelation function,

$$\langle n_1(0) n_1(t) \rangle = \frac{1}{Z} \mathrm{Tr}[\exp(-\beta H) n_1 \exp(iHt/\hbar) \times n_1 \exp(-iHt/\hbar)], \tag{2.7}$$

where n_1 is the population operator for state 1,

$$n_1 = \begin{pmatrix} 1 & 0 & 0 \\ 0 & 0 & 0 \\ 0 & 0 & 0 \end{pmatrix},$$

$\beta = 1/k_B T$, and $Z = \mathrm{Tr} \exp(-\beta H)$. Another measure is the nonequilibrium population, such as

$$\bar{n}_1(t) = \frac{1}{Z_1} \mathrm{Tr}[\exp(-\beta H_1) \exp(iHt/\hbar) n_1 \exp(-iHt/\hbar)], \tag{2.8}$$

where H_1 and Z_1 are the Hamiltonian and the partition function, respectively, for the system constrained to state 1. This quantity describes the relaxation of state 1 after an initial preparation which constrained the system to that charge localized state. When linear response theory is accurate, $\bar{n}_1(t)$ and $\langle n_1(0) n_1(t) \rangle$ exhibit the same time dependence. In general, however, the two functions can be markedly different as some of our results will demonstrate.

III. NUMERICAL METHODS

To carry out the computation of $\bar{n}_1(t)$ and $\langle n_1(0) n_1(t) \rangle$, we employ the path-integral sum representation of the propagators, $\exp(-\beta H)$ and $\exp(\pm iHt/\hbar)$. In particular, we use the standard Trotter formula [12]. The bath is removed from explicit consideration by the method of Gaussian integration. The resulting discretized action is a functional of the spin variable $\sigma^{(i)}$ which labels the state occupied at time slice i ($\sigma^{(i)} = 1, 0$, and -1 correspond to states 1, 2, and 3, respectively). The effect of the bath appears in an influence functional which couples spins at different times. Spins at adjacent time slices are coupled by the action associated with H_0.

The procedure for deriving this representation follows closely the analysis of the symmetric spin-boson model described in Refs. [4,13,14]. Our generalization to three states employs the spin algebra discussed, for example, for the $S = 1$ transverse Ising model in Ref. [15]. The case of a three-level system with one bath has been treated by Egger and Mak [16]. As shown in Appendix A, we find

$$\langle n_1(0) n_1(t) \rangle = \frac{1}{Z} \sum_{\{\sigma^{(i)}\}} \exp[\varphi(\{\sigma_i\})] \times n_1(\sigma^{(p+1)}) n_1(\sigma^{(p+q+1)}), \tag{3.1}$$

where

$$Z = \sum_{\{\sigma_i\}} \exp[\varphi(\{\sigma_i\})]. \tag{3.2}$$

Here p and q are the number of spins on the thermal and time paths, respectively. $\varphi(\{\sigma^{(i)}\})$ is the action given in Appendix A as a function of the classical spins $\sigma^{(i)}$, $i = 1, \ldots, (p + 2q)$, and $n_1(\sigma) = (\sigma + \sigma^2)/2$ is 1 when $\sigma = 1$, and zero otherwise. Similarly,

$$\bar{n}_1(t) = \frac{1}{Z_1} \sum_{\{\sigma_i\}}{}' \exp[\varphi(\{\sigma^{(i)}\})] n_1(\sigma^{(p+q+1)}), \tag{3.3}$$

where Z_1 and the primed summation samples with all $\sigma^{(i)} = 1$ for $1 \le i \le p + 1$.

To evaluate the summations, we can perform either a Monte Carlo simulation or exact numerical enumeration of the paths. In the quantum Monte Carlo simulation, one encounters the sign problem [13,17–23]. There have been several attempts to overcome the situation. Recently, Egger and Mak [19] proposed the optimized filtering method, which reduces the statistical error due to the sign problem. In this paper, we report the exact enumeration, which is free of the sign problem. The limitation of our chosen procedure, of course, is that the computational effort grows exponentially with the number of spins (and thus length of time t). The computational time for Monte Carlo simulation grows as a low power of this number.

In our computer code, we generate spin configurations, calculate the action for each configuration, and add the quantities. The code is suitable for vectorization, because we can use a large vector length by vectorizing with the spin states. Typically, for a two-level system, we used states of 12 spins (4096 states) for the innermost vector loop. The bulk of the CPU time is spent calculating the exponential of action $\varphi(\{\sigma^{(i)}\})$. The details of the algorithm are shown in Ref. [24]. For $N = 27$ spins [$N = p + 2q$ for $\langle n_1(0) n_1(t) \rangle$ or $N = 2q - 1$ for $\bar{n}_1(t)$], the exact enumeration of a two-level system requires the summation of about 10^8 states and takes about 3 min on the Cray X-MP computer at University of California, Berkeley. For short-time behavior in the case of strong electronic coupling (i.e., the coherent or nearly coherent regime) this method is more effective than the stationary-phase Monte Carlo simulation. Deep into the incoherent regime for long times, Monte Carlo simulation would be preferable.

IV. RESULTS

A. Adiabatic case for two-level system

We consider first the limit of an adiabatic bath. Here, the bath influences the tunneling system as a mean field, and the spin correlation functions can be evaluated exactly in terms of simple integrals. The general three-state system is analyzed in Appendix B. A special case is the asymmetric two-state system for which

$$\bar{n}_1(t) = 1 - \frac{K^2}{\sqrt{2\pi\chi}} \int_{-\infty}^{\infty} d\mathcal{E} \exp\left(-\frac{\mathcal{E}^2}{2\chi}\right) \frac{\sin^2(f(\mathcal{E})t/\hbar)}{f(\mathcal{E})^2} \tag{4.1}$$

(see Ref. [6] for the symmetric two-level system) where

$$f(\mathcal{E}) = \left\{ \left(\mathcal{E} + \beta\chi - \frac{E_1}{2}\right)^2 + K^2 \right\}^{1/2} \tag{4.2}$$

and $K = J_{12}$, $\mathcal{E} = \mathcal{E}_{12}$, $c/\beta = \chi = \langle \mathcal{E}^2 \rangle$, $E_2 = 0$, and $J_{23} = J_{13} = 0$. The corresponding diabatic energies are

$$E_+(\mathcal{E}) = \frac{\mathcal{E}^2}{2c} + \mathcal{E} + E_1,$$
$$E_-(\mathcal{E}) = \frac{\mathcal{E}^2}{2c} - \mathcal{E}. \tag{4.3}$$

For three different cases the diabatic surfaces are drawn in Fig. 1. If we look at $\bar{n}_1(t, E_1)$ as a function of E_1, we obtain, from Eq. (4.1) and Eq. (4.2), $\bar{n}_1(t, 2c - \alpha) = \bar{n}_1(t, 2c + \alpha)$. It can be shown that the largest initial oscillation in $\bar{n}_1(t)$ occurs for the case where $E_1 = 2c$. This value of E_1 coincides with the boundary between the normal [e.g., case (a)] and inverted [e.g., case (c)] regions of electron transfer.

The exactly solvable adiabatic bath limit can be used as a basis for comparison to determine the largest acceptable time steps in the Trotter discretization. An example of $\bar{n}_1(t)$ in the adiabatic bath limit is shown in Fig. 2.

B. Phase diagram for asymmetric two-level system

In this subsection, we investigate the asymmetric two-level system in the Ohmic bath of Eq. (2.6). The results

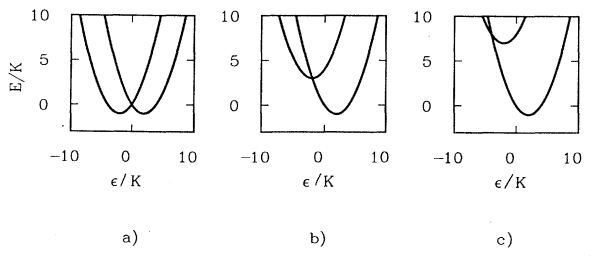

FIG. 1. Diabatic surfaces for the adiabatic case of $E_1/K = 0, 4, 8$ [(a), (b), (c), respectively] and $\beta K = 1.0$, $c/K^2 = 2.0$, $E_2 = 0$.

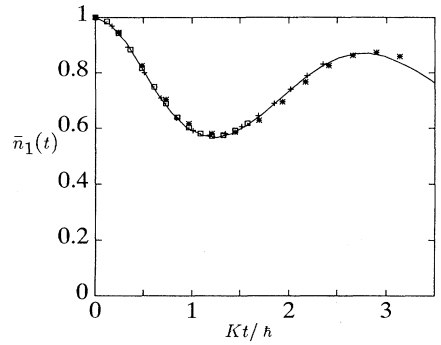

FIG. 2. $\bar{n}_1(t)$ for two-level adiabatic case of $\beta K = 0.4$, $c/K^2 = 0.5$, $E_1/K = 3$, $E_2 = 0$, and $Kt/\hbar = \pi/2$ (□), $3\pi/4$ (+), π (*). The solid line is the exact result obtained from Eq. (4.1).

were obtained by exact enumerations of the paths. We set $\eta_{AA} = \eta$ and $\omega_{AA}^{(c)} = \omega^{(c)}$. In Fig. 3, we show an example of relaxation as a function of the strength of bath η. Changing η coincides with changing the diabatic surface curvature, $\pi/2\omega^{(c)}\eta$. When η is small, the relaxation shows oscillatory behavior and we call this coherent behavior. When η is large, the relaxation becomes a monotonically decreasing function and we call this incoherent behavior.

In Fig. 4, we show the coherent-incoherent phase diagram obtained by analyzing the relaxation $\bar{n}_1(t)$. At high temperatures, the phase boundary is relatively independent of the asymmetry or driving force E_1. At low temperatures, there is dependence upon E_1. For $k_BT/K > 2.5$, the phase boundary for asymmetric cases $E_1/K = 2$ or -2 lies at smaller η than for the symmetric case $E_1/K = 0$. Around $k_BT/K \sim 2.5$, the phase boundary for $E_1/K = -2$ crosses that for $E_1/K = 0$. Below this temperature, the coherent phase for $E_1/K = -2$ stretches to large η.

At low temperatures, we can see a difference in phase boundary between the two cases $E_1/K = 2$ and $E_1/K = -2$. For example, at $k_BT/K = 1$ and $\eta/\hbar = 0.8$ in Fig. 4, the case $E_1/K = 2$ gives incoherent behavior while $E_1/K = -2$ gives coherent behavior. This means

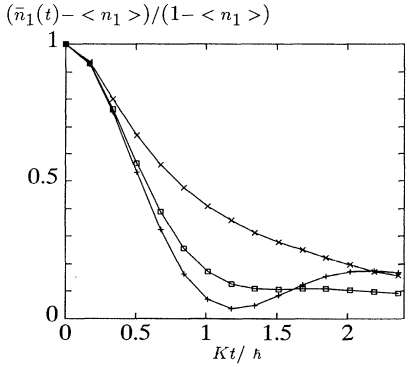

FIG. 3. Relaxation $[\bar{n}_1(t) - \langle n_1 \rangle]/(1 - \langle n_1 \rangle)$ for $\eta/\hbar = 0.1, 0.18, 0.5$ (+,□,×), $E_1/K = -2$, $E_2 = 0$, $\hbar\omega_c/K = 2.5$, $kT/K = 7.5$.

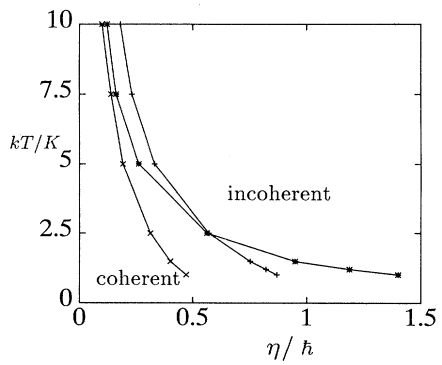

FIG. 4. The phase diagram of the asymmetric two-level system for $\hbar\omega_c/K = 2.5$, and $E_1/K = 2, 0, -2$ ($\times$, $+$, $*$).

that, if two diabatic states under these conditions are separated by a driving force of $2K$, going from the lower to the higher state occurs coherently, while going from the higher to the lower state occurs incoherently. Notice that this asymmetric behavior is a nonlinear effect. In the linear regime, the time correlation function expression for $\bar{n}_1(t)$ would predict a symmetric time dependent behavior as $\bar{n}_1(t) \sim 1 - \bar{n}_2(t)$. Specifically, $\bar{n}_1(t) - \langle n_1 \rangle$ is proportional to a complex time integral of $\langle \delta n_1(0) \delta n_1(t) \rangle$, $[\delta n_1(t) = n_1(t) - \langle n_1 \rangle]$; this autocorrelation function is identical to $\langle \delta n_2(0) \delta n_2(t) \rangle$. Thus the quantity $\bar{n}_1(t)$ contains some properties that are averaged out in $\langle n_1(0) n_1(t) \rangle$.

C. Relaxation in the incoherent phase

In this subsection, we compare the normal region and inverted region in the incoherent phase. In this comparison, we confine our examination to those regions of parameter space where our limited range of time ($t_{\max} = q\Delta t$, $q = 14$, i.e., 14 Trotter time steps) is still reasonably long. The results were obtained by exact enumerations. In Fig. 5 we show relaxation for different values of E_1. In Fig. 6, we analyze the functional form of the relaxation of Fig. 5. In the normal region, we see that the relaxation occurs as a power law; while in the inverted region, it occurs as an exponential. The power-law relaxation can be interpreted as an intermediate behavior between coherent relaxation and exponential relaxation. In the normal region, we calculated the power ν in

$$\bar{n}_1(t) - \langle n_1 \rangle \sim A \quad t^{-\nu}, \tag{4.4}$$

where A and ν are constants independent of time t. The power ν is plotted as a function of energy E_1 in Fig. 7(a). As the driving force becomes larger, the exponent ν becomes larger and the relaxation becomes faster until the system reaches the inverted region.

In the inverted region, we fit the following equation to the relaxation:

$$\bar{n}_1(t) - \langle n_1 \rangle \sim A' \exp(-t/\tau). \tag{4.5}$$

Here, A' and τ are constants independent of time t. The time constant τ is plotted as a function of energy E_1 in Fig. 7(b). As the energy E_1 is increased, τ increases and the relaxation becomes slower.

As we can see in these results, we have different types of relaxation in the normal region and the inverted region. The case of small electronic coupling K is most often considered in the theory of electron transfer [1,2]. Here, we are dealing with the case of strong electronic coupling K. The strong electronic coupling gives power-law behavior for the relaxation of the population function.

From the time constant τ, we get the rate constant

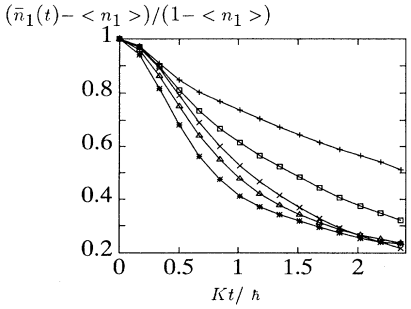

FIG. 5. $\bar{n}_1(t)$ for an asymmetric two-state system in a bath with $\beta K = 1.0$, $\hbar\omega_c/K = 2.5$, $\eta/\hbar = 1.2566$, and $E_1/K = 7, 5, 3, 1, 0$ ($+$, $\square$, $\times$, $\triangle$,$*$) obtained by exact enumeration.

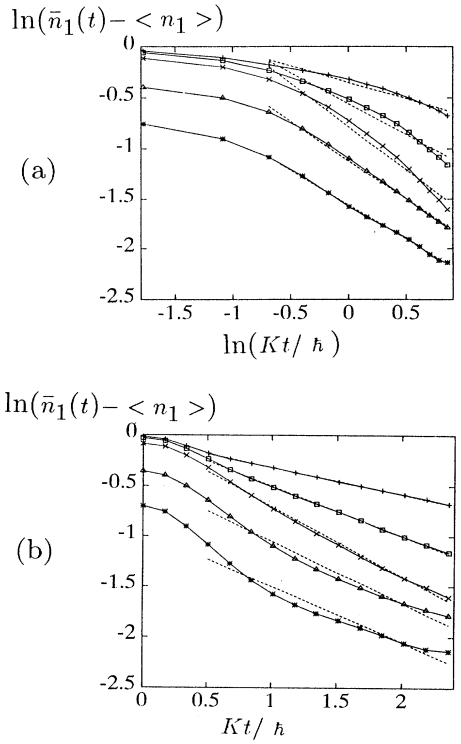

FIG. 6. $\ln[\bar{n}_1(t) - \langle n_1 \rangle]$ as a function of (a) $\ln t$ and (b) t, for an asymmetric two-state system in a bath with $\beta K = 1.0$, $\hbar\omega_c/K = 2.5$, $\eta/\hbar = 1.2566$, and $E_1/K = 7, 5, 3, 1, 0$ ($+$, $\square$, $\times$, $\triangle$,$*$) obtained by exact enumeration. The dashed line is obtained by fitting the last 12 points to a straight line.

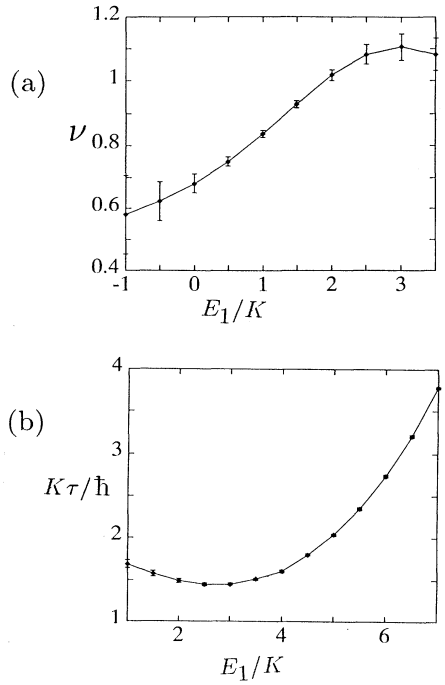

FIG. 7. (a) The exponent ν for the power-law decay and (b) the time constant τ for the exponential decay as a function of energy E_1 for an asymmetric two-state system in a bath with $\beta K = 1.0$, $\hbar\omega_c/K = 2.5$, $\eta/\hbar = 1.2566$. As shown in Fig. 6, we fitted the last 12, 11, or 10 points to a straight line, obtained ν or τ for each case, and calculated the average and the standard deviation from those three sets of data.

$k = 1/\tau$. In Fig. 8, we plot the rate constant k as a function of the energy E_1 and compare it with the rates predicted by classical and quantal golden rate formulas. In the normal region, our results show that the relaxation is not exponential. The rate constant is therefore not perfectly defined, and error bars indicate as such in the inverted region. The driving force that gives the maximum rate of transfer shifts to around $E_1/K = 2.7$, as opposed to $E_1/K = 4$ predicted from classical theory — the intersection of diabatic surfaces. Both the quantal golden rule calculation and our results give the shifting of the peak to a smaller value of E_1. However, the golden rule calculation overestimates the rate constant for the strong-coupling case, as shown in Fig. 8.

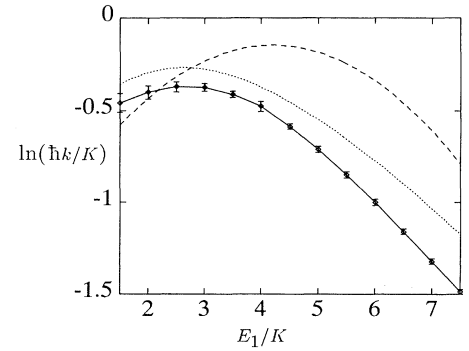

FIG. 8. The rate constant k as a function of energy E_1 for an asymmetric two-state system in a bath with $\beta K = 1.0$, $\hbar\omega_c/K = 2.5$, $\eta/\hbar = 1.2566$. The dotted line is the rate constant obtained from the quantum mechanical golden rule calculation employing the formulas of van Duyne and Fischer [30]. The dashed line is obtained from those formulas in the classical limit for the bath.

D. The effect of the third state

To look at the effect of the third state, we have performed an exact calculation on the three-level model. (For other studies on three-level models, see, for example, Refs. [16] and [25].) In Fig. 9, we show some examples of the relaxation of the three-level model for different values of E_2. Here, the number of time slices is $q = 9$. We checked the convergence by performing the calculations with different values of Δt.

From Fig. 9, one can see that the rate becomes slower as E_2 is increased. Panel (c) refers to the case where transfer flows from state 1 to state 3, with state 2 being an intermediate of higher energy. This particular juxtaposition of states may be relevant to the primary charge

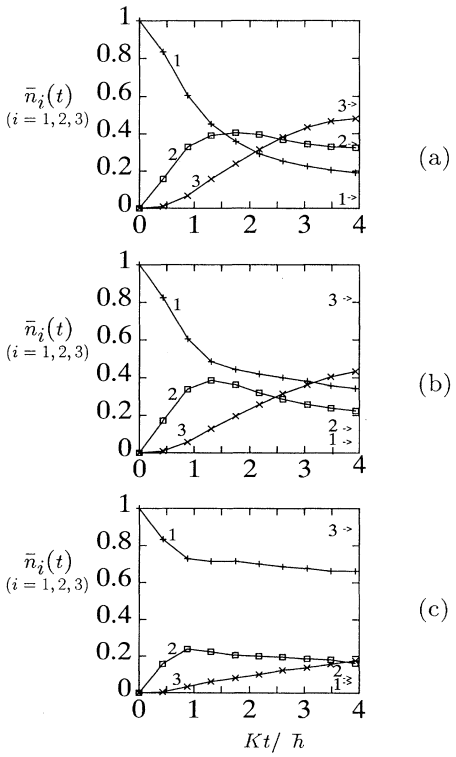

FIG. 9. Relaxation of three-level system with $\beta K = 1$, $\eta^{(AA)}/\hbar = \eta^{(BB)}/\hbar = 0.6$, $\eta^i = 0$ for other i. $\hbar\omega_c^{(AA)}/K = \hbar\omega_c^{(BB)}/K = 2.5$. $E_1/K = 3$, $E_3/K = 0$, $J_{12}/K = J_{23}/K = -1, J_{13}/K = 0$. (a) $E_2/K = 1$, (b) $E_2/K = 3$, and (c) $E_2/K = 5$. The relaxations $\bar{n}_1(t)$, $\bar{n}_2(t)$, and $\bar{n}_3(t)$ are denoted by +, □, and ×, respectively. Arrows indicate the values $\bar{n}_i(t)$ acquire when finally equilibrated.

transfer step of photosynthesis [11,26], although the coupling constant in our simulation is very large. Simple superexchange theory [1] in which state 2 is a virtual intermediate is not sufficient to describe the dynamics shown in Fig. 9. The superexchange perturbation treatment is valid through second order in $K/(E_2-E_1)$. State 2, however, has a significant population at intermediate terms. This population follows from contributions to the dynamics of the order of $[K/(E_2-E_1)]^4$ and higher.

Photosynthesis has also been studied by Egger and Mak [16]. They looked at much smaller coupling constants than our simulation. Our large coupling gives a smaller time scale. (For room temperature $T=300$, the time scale $t=4$ corresponds to about 0.6 ps, which is shorter than the typical electron transfer rate 3 ps [26] in photosynthetic bacteria.) Also, Egger and Mak are looking at the incoherent region, whereas our simulation shows coherent behavior for $\bar{n}_2$.

We have also studied the case with $K_{13}\neq 0$, and the phase diagram is shown in Fig. 10. This corresponds to a simple case of multiple pathways (state $1\rightarrow 2$ or $1\rightarrow 2\rightarrow 3$). The pathways for cytochrome c have been studied by Regan *et al.* [27]. Of course, our coupling constant is too strong for proteins. As has been pointed out by Kostić *et al.* [28], the strong-coupling case can be found in charge transfer in solids, for example, hydrogen tunneling in metals [29].

The phase diagram in Fig. 10 is determined by the behavior of $\bar{n}_1(t)$. The basic behavior concerning η is similar to the case of the two-level system: for small η we have a coherent region, and for large η we have an incoherent region. The effect of E_3 is that, if E_3 is close to E_1 and E_2, we have the coherent region, and if E_3 is farther away from E_1 and E_2, we have the incoherent region. The phase boundary in the region $3\leq E_3/K\leq 4$ is not clear since the oscillation periods of the coherent states are longer than those with other values of E_3. It would be interesting to study the phase diagram with respect to other parameters such as J_{12} and ω_c.

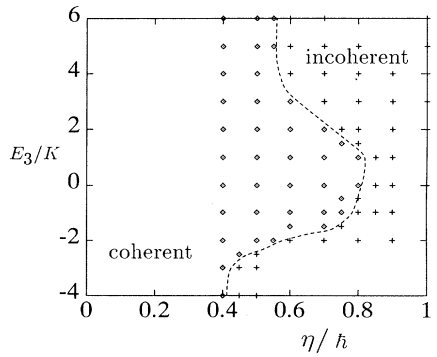

FIG. 10. Phase diagram determined by the behavior of $\bar{n}_1(t)$ for three-level system with $\beta K=1$, $\eta\equiv\eta^{(AA)}=\eta^{(BB)}=0.4\hbar$, $\eta^i=0$ for other i. $\hbar\omega_c^{(AA)}/K=\hbar\omega_c^{(BB)}/K=2.5$. $E_1/K=3$, $E_2/K=0$, $J_{12}=J_{23}=J_{13}=-K$. $\diamond$ denotes the coherent region and $+$ denotes the incoherent region. The dashed line is an approximate phase boundary.

V. SUMMARY AND FUTURE PROBLEMS

We investigated the asymmetric two-level system. We obtained the phase boundary for the coherent-incoherent transition in the case of the asymmetric two-level model. At high temperatures, the asymmetry destroys coherence and we observed a smaller coherent phase than in the symmetric case. At low temperatures, the transition from the low energy state to the high energy state becomes very slow and we observe a large coherent phase. In the incoherent phase, if the electronic coupling is large, the relaxation follows a power law in the normal region and an exponential law in the inverted region.

In this paper, we did not treat the cases of small or intermediate electronic coupling. These cases are interesting in terms of long-distance electron transfer including photosynthesis. Also of interest is the case of other kinds of spectral density, for example, electrons in solids. The super-Ohmic and sub-Ohmic cases should also be investigated in the future.

ACKNOWLEDGMENTS

I would like to thank Professor David Chandler for suggestions and support throughout this research. I would also like to thank John N. Gehlen and Chi Mak for helpful discussions and Jerry Berkman for his advice on the Cray codes. This research was supported by the National Science Foundation (Grant No. CHE-9006235), the Sumitomo Foundation, and a Grant-in-Aid from the Japanese Ministry of Education, Science and Culture. Most of the numerical calculations were done on the Cray X-MP at the University of California, Berkeley, the Cray Y-MP8 at the San Diego Supercomputer Center, and at the Supercomputer Laboratory, Institute for Chemical Research, Kyoto University.

APPENDIX A: ACTION FOR THREE-LEVEL SYSTEM

In this Appendix, we derive the action φ for a three-level system coupled to the Gaussian bath. Starting with Eq. (2.7), we apply the Trotter formula [12] and obtain the following path-integral sum representation of the correlation function:

$$\langle n_1(0)n_1(t)\rangle=\frac{1}{Z}\tilde{\sum}B^{(1)}\cdots B^{(N)}\ n_1(\sigma^{(p+1)})\times n_1(\sigma^{(p+q+1)}),\tag{A1}$$

where p and q are the numbers of spins on the thermal and time paths, respectively, and $N=p+2q$. $n_1(\sigma)=(\sigma^2+\sigma)/2$. $\tilde{\sum}$ is the summation over the spin states and the integration over the bath degrees of freedom:

$$\tilde{\sum}=\sum_{\{\sigma^{(i)}\}}\int\cdots\int\prod_{i=1}^{N}\prod_{j=0}^{\infty}dx_j^{(i)}.\tag{A2}$$

B_i is the product of the matrix elements of the exponen-

tial operators of the Hamiltonian:

$$B^{(i)} = b_0^{(i)}\, b_B^{(i)}\, b_{\rm int}^{(i)}, \tag{A3}$$

and

$$\begin{aligned} b_0^{(i)} &= \langle \sigma^{(i-1)} | \exp(-\Delta^{(i)} H_0) | \sigma^{(i)} \rangle, \\ b_B^{(i)} &= \langle X^{(i-1)} | \exp(-\Delta^{(i)} H_B) | X^{(i)} \rangle, \\ b_{\rm int}^{(i)} &= \langle \sigma^{(i)}, X^{(i)} | \exp(-\Delta^{(i)} H_{\rm int}) | \sigma^{(i)}, X^{(i)} \rangle, \end{aligned} \tag{A4}$$

where $X^{(i)} = (x_1^{(i)}, x_2^{(i)}, \ldots, x_j^{(i)}, \ldots)$ and

$$\Delta^{(i)} = \begin{cases} \frac{\beta}{p} & \text{if} \quad i = 1, \ldots, p \\ \frac{-it}{\hbar q} & \text{if} \quad i = p+1, \ldots, p+q \\ \frac{it}{\hbar q} & \text{if} \quad i = p+q+1, \ldots, N. \end{cases} \tag{A5}$$

Due to the trace in Eq. (2.7), we have cyclic conditions on the spin and bath coordinates: $\sigma^{(0)} = \sigma^{(N)}$, $X^{(0)} = X^{(N)}$. Z in Eq. (A1) is the path-integral representation of the partition function:

$$Z = \tilde{\sum} B^{(1)} \cdots B^{(N)}. \tag{A6}$$

We can rewrite $H_{\rm int}$ in the form

$$H_{\rm int} = \sum_k \mathcal{E}_k f_k(\sigma^{(i)}), \tag{A7}$$

where

$$\begin{aligned} f_A(\sigma) &= \frac{3\sigma^2 + \sigma - 2}{2}, \\ f_B(\sigma) &= -\sigma, \\ f_C(\sigma) &= -\frac{3\sigma^2 - \sigma - 2}{2}. \end{aligned} \tag{A8}$$

Then,

$$b_{\rm int}^{(1)} \cdots b_{\rm int}^{(N)} = \exp\left(-\sum_{ijk} \Delta^{(i)} c_{jk} f_k(\sigma^{(i)}) x_j^{(i)} \right). \tag{A9}$$

Now, we make use of the following property of Gaussian integrals:

$$\left\langle \exp\left(\sum_j d_j x_j \right) \right\rangle_B = \exp\left(\frac{1}{2} \sum_j \sum_{j'} d_j d_{j'} \langle x_j x_{j'} \rangle_B \right), \tag{A10}$$

where the average $\langle\,\rangle_B$ is the integration with Gaussian weights in x_j, and $\langle x_j \rangle_B = 0$. In our case,

$$\langle\,\rangle_B \propto \int \cdots \int dx_1 \cdots dx_N b_B^{(1)} \cdots b_B^{(N)}. \tag{A11}$$

Then,

$$\langle b_{\rm int}^{(1)} \cdots b_{\rm int}^{(N)} \rangle_B = \exp(\varphi_{\rm int}), \tag{A12}$$

where

$$\varphi_{\rm int} = \frac{1}{2} \sum_{ijk} \sum_{i'j'k'} \Delta^{(i)} \Delta^{(i')} c_{jk} c_{j'k'} f_k(\sigma^{(i)}) f_{k'}(\sigma^{(i')}) \times \langle x_j^{(i)} x_{j'}^{(i')} \rangle_B. \tag{A13}$$

We substitute the following correlation function for the harmonic oscillators:

$$\langle x_j^{(i)} x_j^{\prime(i')} \rangle_B = \frac{\delta_{jj'} \hbar}{2 m_j \omega_j} \frac{\cosh\left[\hbar \omega_j (\Delta^{(ii')} - \Delta^{(i'i)})/2 \right]}{\sinh(\beta \hbar \omega_j / 2)}, \tag{A14}$$

where we use, as in Ref. [13],

$$\Delta^{(ii')} = \sum_{m=i}^{i'-1} \Delta^{(m)}. \tag{A15}$$

Now $\varphi_{\rm int}$ can be written as

$$\begin{aligned} \varphi_{\rm int} = \frac{1}{2} \sum_{ii'} \Delta^{(i)} \Delta^{(i')} \{ & P_1^{(ii')} \sigma^{(i)^2} \sigma^{(i')^2} \\ & + P_2^{(ii')} \sigma^{(i)^2} \sigma^{(i')} + P_3^{(ii')} \sigma^{(i)} \sigma^{(i')} \\ & + P_4^{(ii')} \sigma^{(i)^2} + P_5^{(ii')} \sigma^{(i)} \}, \end{aligned} \tag{A16}$$

where, omitting i, i' for simplicity,

$$\begin{aligned} P_1 &= \frac{9}{4}\chi_{AA} + \frac{9}{4}\chi_{BB} - \frac{9}{2}\chi_{AB}, \\ P_2 &= \frac{3}{2}\chi_{AA} - \frac{3}{2}\chi_{BB} - 3\chi_{AC} + 3\chi_{BC}, \\ P_3 &= \frac{1}{4}\chi_{AA} + \frac{1}{4}\chi_{BB} + \chi_{CC} - \chi_{AC} + \frac{1}{2}\chi_{AB} - \chi_{BC}, \\ P_4 &= -3\chi_{AA} + 3\chi_{BB} + 6\chi_{AB}, \\ P_5 &= -\chi_{AA} + \chi_{BB} + 2\chi_{AC} - 2\chi_{BC}. \end{aligned} \tag{A17}$$

Here, χ is obtained by integrating the spectral density:

$$\begin{aligned} \chi_{kk'}^{(ii')} &= \langle \mathcal{E}_k(t^{(i)}) \mathcal{E}_{k'}(t^{(i')}) \rangle \\ &= \frac{\hbar}{\pi} \int_0^\infty J_{kk'}(\omega) \frac{\cosh[\hbar\omega(\Delta^{(ii')} - \Delta^{(i'i)})/2]}{\sinh(\beta\hbar\omega/2)}\, d\omega. \end{aligned} \tag{A18}$$

This integral can be expressed by gamma functions [18].

Using $\varphi_{\rm int}$, the correlation function of Eq. (A1) takes the form

$$\begin{aligned} \langle n_1(0) n_1(t) \rangle \propto \sum_{\{\sigma^{(i)}\}} & b_0^{(1)} \cdots b_0^{(N)} \exp(\varphi_{\rm int}) \\ & \times n_1(\sigma^{(p+1)}) n_1(\sigma^{(p+q+1)}). \end{aligned} \tag{A19}$$

The matrix elements $b_0^{(i)}$ can be written in terms of the spin variables $\sigma^{(i)}$. Suppose we have a 3×3 symmetric matrix as follows:

$$M = \begin{pmatrix} a_1 & a_2 & a_3 \\ a_2 & a_4 & a_5 \\ a_3 & a_5 & a_6 \end{pmatrix}. \tag{A20}$$

Since $\sigma^3 = \sigma$, we may express M in the form

$$M = \exp(\alpha_1\rho_1 + \alpha_2\rho_2 + \alpha_3\rho_3 + \alpha_4\rho_4 + \alpha_5\rho_5 + \alpha_6\rho_6), \tag{A21}$$

where $\alpha_i = \ln(a_i)$ and the ρ_i's are bilinear algebraic functions of σ, σ^2, σ', σ'^2:

$$\begin{aligned}
\rho_1 &= \frac{1}{4}(\sigma^2\sigma'^2 + \sigma^2\sigma' + \sigma\sigma'^2 + \sigma\sigma'),\\
\rho_2 &= -\sigma^2\sigma'^2 - \frac{1}{2}(\sigma^2\sigma' + \sigma\sigma'^2 - \sigma^2 - \sigma'^2 - \sigma - \sigma'),\\
\rho_3 &= \frac{1}{2}(\sigma^2\sigma'^2 - \sigma\sigma'),\\
\rho_4 &= \sigma^2\sigma'^2 - \sigma^2 - \sigma'^2 + 1,\\
\rho_5 &= -\sigma^2\sigma'^2 + \frac{1}{2}(\sigma^2\sigma' + \sigma\sigma'^2 + \sigma^2 + \sigma'^2 - \sigma - \sigma'),\\
\rho_6 &= \frac{1}{4}(\sigma^2\sigma'^2 - \sigma^2\sigma' - \sigma\sigma'^2 + \sigma\sigma').
\end{aligned} \tag{A22}$$

With this observation in mind, we write

$$b_0^{(1)} \cdots b_0^{(N)} \propto \exp(\varphi_0), \tag{A23}$$

where one may show that

$$\begin{aligned}
\varphi_0 = \frac{1}{2}\sum_i \Big\{ & A_1^{(i)}\sigma^{(i)^2}\sigma^{(i+1)^2}\\
& + A_2^{(i)}(\sigma^{(i)^2}\sigma^{(i+1)} + \sigma^{(i)}\sigma^{(i+1)^2})\\
& + A_3^{(i)}\sigma^{(i)}\sigma^{(i+1)} + A_4^{(i)}\sigma^{(i)^2} + A_5^{(i)}\sigma^{(i)}\Big\}.
\end{aligned} \tag{A24}$$

Here, the coefficients are expressed by the matrix elements of the bare Hamiltonian H_0 in Eq. (2.2):

$$\begin{aligned}
A_1^{(i)} &= \frac{e_{11}^{(i)}}{4} + e_{22}^{(i)} + \frac{e_{33}^{(i)}}{4} - e_{12}^{(i)} - e_{23}^{(i)} + \frac{e_{13}^{(i)}}{2},\\
A_2^{(i)} &= \frac{e_{11}^{(i)}}{4} - \frac{e_{33}^{(i)}}{4} - \frac{e_{12}^{(i)}}{2} + \frac{e_{23}^{(i)}}{2},\\
A_3^{(i)} &= \frac{e_{11}^{(i)}}{4} + \frac{e_{33}^{(i)}}{4} - \frac{e_{13}^{(i)}}{2},\\
A_4^{(i)} &= -2e_{22}^{(i)} + e_{12}^{(i)} + e_{23}^{(i)},\\
A_5^{(i)} &= e_{12}^{(i)} - e_{23}^{(i)},
\end{aligned} \tag{A25}$$

with

$$e_{kl}^{(i)} = \ln\left[(b_0^{(i)})_{kl}\right]. \tag{A26}$$

φ_0 is the action for the bare Hamiltonian H_0. The full action is

$$\varphi = \varphi_0 + \varphi_{\rm int}. \tag{A27}$$

APPENDIX B: ADIABATIC CASE FOR THREE-LEVEL SYSTEM

For the case of a nondynamical adiabatic bath, quantities such as Eq. (2.7) and Eq. (2.8) can be evaluated in terms of quadrature. The derivation can be carried out entirely within the context of Hamiltonian mechanics. Nevertheless, it is instructive to carry out the derivation from the path-integral perspective.

For the adiabatic case, the correlations of electric fields are independent of time. In the absence of cross correlations, we let

$$\langle \mathcal{E}_k(t)\mathcal{E}_{k'}(t')\rangle = \begin{cases} \chi_A & \text{if} \quad k = k' = A\\ \chi_B & \text{if} \quad k = k' = B\\ \chi_C & \text{if} \quad k = k' = C\\ 0 & \text{otherwise,} \end{cases} \tag{B1}$$

where $\chi_k > 0$ $(k = A, B, C)$. Then the interaction part of the action φ in Eq. (A16) takes the form

$$\varphi_{\rm int} = Q_1 S_2^2 + Q_2 S_2 S_1 + Q_3 S_1^2 + Q_4 S_2 + Q_5 S_1, \tag{B2}$$

where

$$S_1 = \sum_i \Delta_i\sigma_i, \quad S_2 = \sum_i \Delta_i\sigma_i^2, \tag{B3}$$

and Q_i is expressed by

$$\begin{aligned}
Q_1 &= \frac{9}{8}\chi_A + \frac{9}{8}\chi_B,\\
Q_2 &= \frac{3}{4}\chi_A - \frac{3}{4}\chi_B,\\
Q_3 &= \frac{1}{8}\chi_A + \frac{1}{8}\chi_B + \frac{1}{2}\chi_C,\\
Q_4 &= -\frac{3}{2}(\chi_A + \chi_B)\beta,\\
Q_5 &= -\frac{1}{2}(\chi_A + \chi_B)\beta.
\end{aligned} \tag{B4}$$

To use the following Gaussian integral:

$$\exp\left(\frac{a_1 S_1^2}{2}\right) = \frac{1}{\sqrt{2\pi a_1}}\int_{-\infty}^{\infty} d\mathcal{E}_1 \exp\left(-\frac{\mathcal{E}_1^2}{2a_1} - \mathcal{E}_1 S_1\right), \tag{B5}$$

we transform Eq. (B2) into the form

$$\begin{aligned}
\varphi_{\rm int} = {} & Q_1(S_2 + \frac{Q_2}{2Q_1}S_1)^2 + (Q_3 - \frac{Q_2^2}{4Q_1})S_1^2\\
& + Q_4 S_2 + Q_5 S_1.
\end{aligned} \tag{B6}$$

Thus,

$$\begin{aligned}
\exp(\varphi_{\rm int}) = {} & \int\int \frac{d\mathcal{E}_1 d\mathcal{E}_2}{2\pi\sqrt{a_1 a_2}} \exp\left(-\frac{\mathcal{E}_1^2}{2a_1} - \frac{\mathcal{E}_2^2}{2a_2}\right)\\
& \times \exp\left\{-\left(\frac{Q_2}{2Q_1}\mathcal{E}_2 + \mathcal{E}_1 - Q_5\right) S_1\right\}\\
& \times \exp\{-(\mathcal{E}_2 - Q_4)S_2\},
\end{aligned} \tag{B7}$$

where it is understood that the unlabeled integrations are from $-\infty$ to ∞, and

$$\begin{aligned}
a_1 &= 2\left(Q_3 - \frac{Q_2^2}{4Q_1}\right),\\
a_2 &= 2Q_1.
\end{aligned} \tag{B8}$$

One may show that both a_1 and a_2 are positive. Finally,

for the three-level model, we obtain

$$\langle n_1(0)n_1(t)\rangle = \frac{1}{Z_{3a}}\int\int \frac{d\mathcal{E}_1 d\mathcal{E}_2}{2\pi(a_1a_2)^{1/2}} \exp\left(-\frac{\mathcal{E}_1^2}{2a_1}-\frac{\mathcal{E}_2^2}{2a_2}\right) \times \mathrm{Tr}\left[\exp(-\beta H')n_1 \exp\left(\frac{iH't}{\hbar}\right) \times n_1 \exp\left(-\frac{iH't}{\hbar}\right)\right], \tag{B9}$$

where the Hamiltonian H' is described by the equation

$$H' = H_0 + \left(\frac{Q_2}{2Q_1}\mathcal{E}_2 - \mathcal{E}_1 - Q_5\right)\sigma + (\mathcal{E}_2 - Q_4)\sigma^2, \tag{B10}$$

and

$$Z_{3a} = \int\int \frac{d\mathcal{E}_1 d\mathcal{E}_2}{2\pi\sqrt{a_1a_2}} \exp\left(-\frac{\mathcal{E}_1^2}{2a_1}-\frac{\mathcal{E}_2^2}{2a_2}\right) \times \mathrm{Tr}\exp(-\beta H'). \tag{B11}$$

The trace operation in Eq. (B9) is most readily performed numerically by first diagonalizing H' and evaluating the matrix elements of n_1 in that representation.

As a special case, consider the expression for an asymmetric two-level system. We use the states $\sigma = 1$ and -1, and set $\chi_A = \chi_B = 0$, $\chi_C = \chi$. This gives $Q_1 = Q_2 = Q_4 = Q_5 = 0$ and $Q_3 = \chi/2$ in Eq. (B4). The parameters in Eq. (B8) become $a_1 = \chi$ and $a_2 = 0$. The Gaussian function of $\mathcal{E}_2$ in Eq. (B9) approaches the δ function $\delta(\mathcal{E}_2)$ as a_2 approaches zero. If we let $\mathcal{E}_1 = \mathcal{E}$, the correlation function for an asymmetric two-level system becomes

$$\langle n_1(0)n_1(t)\rangle = \frac{1}{Z_{2a}}\int d\mathcal{E}\exp(-\frac{\mathcal{E}^2}{2\chi}) \times \mathrm{Tr}\left[\exp(-\beta H')n_1 \exp\left(\frac{iH't}{\hbar}\right) \times n_1 \exp\left(-\frac{iH't}{\hbar}\right)\right], \tag{B12}$$

where the Hamiltonian H' is now described by the equation

$$H' = H_0 - \mathcal{E}\sigma, \tag{B13}$$

and

$$Z_{2a} = \int d\mathcal{E}\exp\left(-\frac{\mathcal{E}^2}{2\chi}\right)\mathrm{Tr}\exp(-\beta H'). \tag{B14}$$

Employing Eq. (B13), we obtain

$$Z_{2a} = \int d\mathcal{E}[\exp(-\beta E_+) + \exp(-\beta E_-)], \tag{B15}$$

where

$$E_\pm = \frac{\mathcal{E}^2}{2\chi} + \frac{E_1 \pm \sqrt{(E_1 - 2\mathcal{E})^2 + 4K^2}}{2}. \tag{B16}$$

Setting $K = 0$, we obtain the diabatic energies as in Eq. (4.3). The adiabatic $\bar{n}_1(t)$ is obtained similarly:

$$\bar{n}_1(t) = \frac{\exp(-\beta^2\chi/2)}{(2\pi\chi)^{1/2}}\int d\mathcal{E}\exp\left(-\frac{\mathcal{E}^2}{2\chi}-\beta\mathcal{E}\right) \times \langle 1|\exp(iH't)n_1\exp(-iH't)|1\rangle, \tag{B17}$$

where H' is the same as in Eq. (B13). Employing the eigenstates and eigenvalues of the 2×2 Hermitian matrix H' and shifting $\mathcal{E}$ by $\chi\beta$, one obtains, for example, Eq. (4.1) from Eq. (B17).

[1] J. Ulstrup, *Charge Transfer Processes in Condensed Media* (Springer, New York, 1979); R. A. Marcus and N. Sutin, Biochim. Biophys. Acta **811**, 265 (1985).

[2] R. A. Marcus, J. Am. Chem. Soc. **24**, 966 (1956); P. Siders and R. A. Marcus, *ibid.* **103**, 741 (1981). J. Chem. Phys. **91**, 281 (1989); A. Yoshimori and T. Kakitani, J. Phys. Soc. Jpn. **61**, 2577 (1992).

[3] N. Liang, J. R. Miller, and G. L. Closs, J. Am. Chem. Soc. **112**, 5353 (1990); E. Akesson *et al.*, J. Chem. Phys. **96**, 7859 (1992).

[4] D. Chandler, in *Liquids, Freezing and Glass Transition*, Proceedings of the School of Theoretical Physics, Les Houches, 1989, edited by J. P. Hansen, D. Levesque, and J. Zinn-Justin (North Holland, New York, 1991), Sec. LI.

[5] A. J. Leggett, S. Chakravarty, A. T. Dorsey, M. P. A. Fisher, A. Garg, and W. Zwerger, Rev. Mod. Phys. **59**, 1 (1987).

[6] B. Carmeli and D. Chandler, J. Chem. Phys. **82**, 3400 (1985).

[7] J. S. Bader and D. Chandler, Chem. Phys. Lett. **157**, 501 (1989); J. S. Bader, R. A. Kuharski, and D. Chandler, J. Chem. Phys. **93**, 230 (1990).

[8] A. Warshel and J.-K. Hwang, J. Chem. Phys. **84**, 4938 (1986).

[9] M. Maroncelli and G. R. Freming, J. Chem. Phys. **86**, 6221 (1987).

[10] E. A. Carter and J. T. Hynes, J. Chem. Phys. **94**, 5961 (1991).

[11] M. Marchi, J. N. Gehlen. D. Chandler, and M. Newton, J. Am. Chem. Soc. **115**, 4178 (1993); J. N. Gehlen, M. Marchi, and D. Chandler, Science **263**, 499 (1994).

[12] H. F. Trotter, Proc. Am. Math. Soc. **10**, 545 (1959); M. Suzuki, Phys. Lett. **113A**, 299 (1985).

[13] C. H. Mak and D. Chandler, Phys. Rev. A **41**, 5709 (1990); **44**, 2352 (1991); C. H. Mak, Phys. Rev. Lett. **68**, 899 (1992).

[14] E. C. Behrman and P. G. Wolynes, J. Chem. Phys. **83**, 5863 (1985).

[15] S. Dai, Q. Jiang, and Z. Li, Phys. Rev. B **42**, 2597 (1990).

[16] R. Egger and C. H. Mak, J. Phys. Chem. **98**, 9903 (1994).

[17] R. Egger and U. Weiss, Z. Phys. B **89**, 97 (1992); U. Weiss, *Quantum Dissipative Systems* (World Scientific, Singapore, 1993).

[18] R. Egger, C. H. Mak, and U. Weiss, J. Chem. Phys. **100**,

2651 (1994).
[19] R. Egger and C. H. Mak, Phys. Rev. B **50**, 15 210 (1994).
[20] M. Takasu and D. Chandler, in *Proceedings of the Workshop of Harmonic Oscillators*, edited by D. Han, Y. S. Kim, and W. W. Zachary, NASA Report No. 3197, 1992, p. 365; in *Computer Aided Innovation of New Materials II*, edited by M. Doyama *et al.* (North-Holland, Amsterdam, 1993), p. 375.
[21] M. Takasu, S. Miyashita, and M. Suzuki, Prog. Theor. Phys. **75**, 1254 (1986); in *Quantum Monte Carlo Methods*, edited by M. Suzuki, Springer Series in Solid State Sciences Vol. 74 (Springer-Verlag, Berlin, 1987), p. 114.
[22] J. D. Doll, R. D. Coalson, and D. L. Freeman, J. Chem. Phys. **87**, 1641 (1987); N. Makri and W. H. Miller, *ibid.* **89**, 2170 (1988).
[23] E. Y. Loh *et al.*, Phys. Rev. B **41**, 9301 (1990); N. Furukawa and M. Imada, J. Phys. Soc. Jpn. **60**, 810 (1991); N. Hatano and M. Suzuki, Phys. Lett. A **163**, 246 (1992); T. Nakamura, N. Hatano, and H. Nishimori, J. Phys. Soc. Jpn. **61**, 3494 (1992).
[24] M. Takasu, in *Quantum Monte Carlo Methods in Condensed Matter Physics*, edited by M. Suzuki (World Scientific, Singapore, 1993), p. 356.
[25] Y. Hu and S. Mukamel, J. Chem. Phys. **91**, 6973 (1989).
[26] S. G. Boxer, Annu. Rev. Biophys. Chem. **19**, 267 (1990); S. Creighton, J.-K. Hwang, A. Warshel, W. W. Parson, and J. Norris, Biochemistry **27**, 774 (1988); A. Warshel, Z.-T. Chu, and W. W. Parson, Science **246**, 112 (1989); W. W. Parson, V. Nagarajan, D. Gaul, C. C. Schenck, Z.-T. Chu, and A. Warshel, in *Reaction Centers of Photosynthetic Bacteria*, edited by M. E. Michel-Beyerle (Springer, Berlin, 1991), p. 239; W. W. Parson, Z.-T. Chu, and A. Warshel, Biochim. Biophys. Acta. **1017**, 251 (1990).
[27] J. J. Regan, S. M. Risser, D. N. Beratan, and J. N. Onuchic, J. Phys. Chem. **97**, 3083 (1993).
[28] D. Kostić, Z. Ivić, D. Kapor, and A. Tančić, J. Phys. Condens. Mater. **6**, 729 (1994).
[29] H. Wipf, A. Magerl, S. M. Shapiro, S. K. Satija, and W. Thomlinson, Phys. Rev. Lett. **46**, 947 (1981).
[30] R. P. Van Duyne and S. F. Fischer, Chem. Phys. **5**, 183 (1974).